Proceedings of the American Control Conference
Philadelphia, Pennsylvania • June 1998

State Space and Transfer Function Modeling of Evanescent Waves in Two-Dimensional Acoustics

Harshad S. Sane, Dennis S. Bernstein *, and Karl Grosh †
The University of Michigan
Ann Arbor, MI 48109-2140
{harshad, dsbaero,grosh}@umich.edu

Abstract

With intense current interest in active noise control, it is desirable to develop models of acoustic phenomena that are useful for state-space-based control methodologies. Consequently, this paper extends the one-dimensional modeling of acoustic transfer functions developed in earlier work to the case of two-dimensional acoustics. This extension must therefore account for the phenomenon of evanescent waves, which are non-propagating and thus affect only the near field. While evanescent waves are well understood within the context of wave models, their presence is less apparent in state space-based model modals. This paper thus presents a derivation of state space models for two-dimensional acoustics which are shown to predict the presence of evanescent waves.

1. Introduction

The study of waves in elastic media is primarily concerned with the spatial characteristics of the response to harmonic inputs and is of fundamental importance in acoustics and structural mechanics [2, 4, 6]. Wave models have been used as the basis for active vibration control [1, 5]. However, the traditional approach to feedback control is to base the analysis and design of controllers on transfer function models of the system.

Transfer function models differ from wave models in two key respects. First, whereas wave models are generally based on the response to harmonic inputs, transfer function models predict structural response in the time domain as well. Secondly, transfer functions predict the response of a structure between fixed locations. Hence, transfer functions do not directly predict the spatial propagation of waves, but can be used to recover the same.

In view of the distinctions between wave propagation and transfer function models, it is of significant interest to understand how certain phenomena that are predicted by one type of model are manifested in the other. In particular, this paper is concerned with the phenomenon of evanescent modes which are of fundamental importance in acoustics and vibrations. Evanescent waves arise from the excitation of waveguide modes below their cutoff frequency in acoustic ducts [4], pp. 218-22, [6], pp. 492-495.

In the near field of an actuator, such as in a colocated sensor-actuator configuration, a sensor may measure the effects of both evanescent and propagating waves, thus affecting the performance. The use of state space models that include these effects can help the controller distinguish between these phenomena. The purpose of this paper is to develop such models for acoustics that capture evanescent wave behavior.

Section 2 summarizes the classical analysis of evanescent waves from a wave modeling point of view. The subsequent sections device a way of modeling these effects in an *acoustic duct* with an end-speaker actuator and with the other end open. The analysis in the closed case being very similar to the open case is not be covered. We then obtain state space model and transfer functions from modal analysis and temporal Laplace transforms and compare for validity with the predictions of wave theory. Parametrizing these models in terms of the output location yields a spatial behavior of the duct which agrees with the classical wave theory.

2. Review of Evanescent Waves

Consider a two-dimensional acoustic duct of semi infinite length and width b with rigid side walls. Let x and y denote the coordinates along and across the acoustic duct respectively. Assuming that there is no mean flow in the duct, the wave equation governing the dynamics of acoustic pressure in the duct is given by

$$p_{tt} - c^2(p_{xx} + p_{yy}) = 0, \qquad (1)$$

where $p(x, y, t)$, denotes acoustic pressure at location (x, y) inside the duct at time t and c is the speed of sound in the medium.

The duct is excited by an harmonic acoustic source of frequency ω (wavelength $\lambda = \frac{2\pi}{\omega}$) at $x = 0$. This suggests a wave pattern consisting of standing waves in the transverse direction y and traveling in x direction. The acoustic pressure response $p(x, y, t)$ of the duct to the excitation can be decomposed as a sum of eigenfunctions of the form [4]

$$p_j(x, y, t) = A_j \cos(k_{yj} y)\, e^{\jmath(\omega t - k_{xj} x)} \qquad (2)$$

*Harshad Sane and Dennis Bernstein are with Dept. of Aerospace Eng.
†Karl Grosh is with Dept. of Mechanical Eng.
‡This research was supported in part by the Air Force Office of Scientific Research under grant F49620-98-1-0037 and the University of Michigan Office of the Vice President for Research.

0-7803-4530-4/98 $10.00 © 1998 AACC

Authorized licensed use limited to: University of Michigan Library. Downloaded on July 06,2010 at 16:07:56 UTC from IEEE Xplore. Restrictions apply.

where $k_{yj} = \frac{j\pi}{b}$. Substituting (2) in the wave equation (1) yields

$$k_{xj}^2 = (\omega/c)^2 - k_{yj}^2 \tag{3}$$

It can be seen from (3) that if $\omega < ck_{yk}$ then k_{xk} is imaginary and $p_k(x,y,t)$ decays exponentially in x. Hence, the *cut-off frequency* of the kth eigenfunction is given by

$$\omega_{\mathrm{co},k} \triangleq \frac{k\pi c}{b}. \tag{4}$$

An eigenfunction is said to be *evanescent* since it does not propagate through the acoustic duct. Consequently, for input frequencies higher than the cut-off frequency, the wave propagates along the duct. Note that all eigenfunctions except the fundamental $p_0(x,y,t)$ have non-zero cut-off frequencies. Thus the fundamental, *if excited*, is always transmitted and can never be evanescent. Setting $k = 1$, we define

$$\omega_{\mathrm{co}} \triangleq \frac{\pi c}{b}. \tag{5}$$

as the global cut-off frequency. Comparing (4) and (5), it can be seen that all the eigenfunctions $p_j(x,y,t)$ for $j > 0$ are evanescent if $\omega \leq \omega_{\mathrm{co}}$.

To further illustrate the phenomenon of evanescent waves, recall the concept of group velocity c_{g} [2, 4, 6] of propagating waves which characterizes a notion of speed of energy propagation along the x direction. The group velocity of $p_k(x,y,t)$, $c_{\mathrm{g}} = c\cos\theta$, where θ is defined by

$$\cos\theta \triangleq \sqrt{1 - \left(\frac{\omega_{\mathrm{co},k}}{\omega}\right)^2}. \tag{6}$$

For $\omega > \omega_{\mathrm{co},k}$, θ denotes the angle between the direction of propagation and the longitudinal direction. If the boundary input frequency is high so that θ is small, then c_{g} is approximately equal to c. As ω decreases or θ increases, the direction of propagation becomes predominantly along the transverse direction rather than along axial direction. When ω reaches the critical value $\omega_{\mathrm{co},k}$, it follows that $\theta = \frac{\pi}{2}$ and thus $c_{\mathrm{g}} = 0$ so that no energy propagates down the duct. This is the well-known cut-off phenomenon.

Furthermore, note that if $\omega \leq \omega_{\mathrm{co}}$ then using (5) the wavelength of the boundary input λ satisfies $\lambda = \frac{c}{f} = \frac{2\pi c}{\omega} \geq \frac{2\pi c}{\omega_{\mathrm{co}}} = 2b$. This shows that if the wavelength of the input λ is greater than the maximum allowable wavelength $2b$, then there is no sound propagation, in which case the wave is said to be 'too big to fit' inside the duct of width b.

3. Two-Dimensional Duct with Commandable Boundary Input

Consider a two-dimensional acoustic duct of length L and width b. Let x be the spatial coordinate along the length of the duct with one end at $x = 0$ and the other at $x = L$, and let y be the spatial coordinate along the width of the duct, with $y = 0$ and $y = b$ the sides of the duct. A speaker (boundary input) with a fixed displacement profile $\psi_{\mathrm{bc}} : [0,b] \to \Re$ is mounted at $x = 0$ and the end $x = L$ is either open or closed. The wave equation (1) describes the acoustic pressure dynamics in the duct.

It can be shown that the velocity potential $\Phi(x,y,t)$ also satisfies (1) where $p(x,y,t)$ and $\Phi(x,y,t)$ are related by Euler's equation $p = -\rho\frac{\partial\Phi}{\partial t}$ [4, 7]. Noting that the particle velocity at a location (x,y) is given by $\vec{v} = \vec{\nabla}\Phi$, the boundary conditions for $p(x,y,t)$ at the speaker end are

$$\begin{aligned}\Phi_x(0,y,t) = V_{\mathrm{bc}}(y,t) = \psi_{\mathrm{bc}}(y)u(t), \quad \text{or}\\ p_x(0,y,t) = -\rho\frac{dV_{\mathrm{bc}}}{dt} = -\rho\psi_{\mathrm{bc}}(y)\dot{u}(t).\end{aligned} \tag{7}$$

where $V_{\mathrm{bc}}(y,t) = \psi_{\mathrm{bc}}(y)u(t)$ is cone velocity of the speaker. The boundary conditions for $p(x,y,t)$ at $x = L$ are

$$p(L,y,t) = 0, \qquad \text{if } x = L \text{ is open.} \tag{8}$$

If the end $x = L$ is closed, then $p_x(L,y,t) = 0$ instead. The boundary conditions on the sides of the duct are given by

$$p_y(x,0,t) = 0, \quad p_y(x,b,t) = 0. \tag{9}$$

However, for (7) and (9) to co-exist on the set of points $\{(0,0),(0,b)\}$, $\psi'_{\mathrm{bc}}(y)$ must vanish on $y = 0$ and $y = b$. The boundary condition (8) neglects the radiation effects due to the nonuniform flow and nonuniform pressure distribution across the open end of the duct. The boundary condition (9) assumes that the walls of the acoustic duct are rigid. Note that the boundary condition (7) is non-homogeneous and time varying. To homogenize the boundary conditions (7)-(9), we define the shifted pressure by $\hat{p}(x,y,t) = p(x,y,t) - U(x,y,t)$, where $U(x,y,t)$ satisfies all the boundary conditions. Hence (1) becomes

$$\hat{p}_{tt} - c^2(\hat{p}_{xx} + \hat{p}_{yy}) = -U_{tt} + c^2(U_{xx} + U_{yy}). \tag{10}$$

The choice of shifting function $U(x,y,t)$ is not unique. We choose

$$U(x,y,t) = L\rho\psi_{\mathrm{bc}}(y)\dot{u}(t)(1 - \frac{x}{L}), \quad \text{if } x = L \text{ is open,} \tag{11}$$

$$U(x,y,t) = \frac{1}{2}L\rho\psi_{\mathrm{bc}}(y)\dot{u}(t)(1 - \frac{x}{L})^2, \text{ if } x = L \text{ is closed.} \tag{12}$$

4. State space model for the speaker-open duct

In this section we derive the state space form for the speaker-open duct. Using the shifting function for the open duct given by (11), equation (10) becomes

$$\begin{aligned}\hat{p}_{tt} - c^2(\hat{p}_{xx} + \hat{p}_{yy}) = -L\rho\psi_{\mathrm{bc}}(y)\,\ddot{u}(t)(1 - \frac{x}{L}) +\\ c^2L\rho\psi'_{\mathrm{bc}}(y)\dot{u}(t)(1 - \frac{x}{L}),\end{aligned} \tag{13}$$

with homogeneous boundary conditions

$$\begin{aligned}\hat{p}_x(0,y,t) = 0, \quad \hat{p}(L,y,t) = 0,\\ \hat{p}_y(x,0,t) = 0, \quad \hat{p}_y(x,b,t) = 0.\end{aligned} \tag{14}$$

Authorized licensed use limited to: University of Michigan Library. Downloaded on July 06,2010 at 16:07:56 UTC from IEEE Xplore. Restrictions apply.

To use separation of variables, let

$$\hat{p}(x,y,t) = \sum_{i=1}^{\infty}\sum_{j=1}^{\infty} q_{ij}(t)V_i(x)W_j(y). \tag{15}$$

The eigenfunctions of (13) with the boundary conditions (14) are given by

$$V_i(x) = \sqrt{\frac{2}{L}}\cos\left[\frac{(2i+1)\pi x}{2L}\right], \quad W_j(y) = \sqrt{\frac{2}{b}}\cos\left[\frac{j\pi y}{b}\right]. \tag{16}$$

Define the modal frequencies ω_{ij} as

$$\omega_{ij} = c\sqrt{\left(\frac{(2i+1)\pi}{2L}\right)^2 + \left(\frac{j\pi}{b}\right)^2}, \quad i,j = 0,1,2,\ldots. \tag{17}$$

Substituting (15) into (13), multiplying by $V_{ok}(x)W_{ol}(y)$ and double integrating over $[0,L]\times[0,b]$ yields

$$\ddot{q}_{kl} + \omega_{kl}^2 q_{kl} = b_{1,kl}\,\ddot{u}(t) + b_{2,kl}\dot{u}(t) \quad k,l = 0,1,2,\ldots. \tag{18}$$

$$b_{1,kl} = -\rho\sqrt{\frac{Lb}{4}}\frac{8L}{(2k+1)^2\pi^2}f_{\mathrm{bc},l},$$
$$b_{2,kl} = c^2\rho\sqrt{\frac{Lb}{4}}\frac{8L}{(2k+1)^2\pi^2}g_{\mathrm{bc},l}, \tag{19}$$

where $f_{\mathrm{bc},l}$ and $g_{\mathrm{bc},l}$ are lth Fourier coefficients of the cosine series of $\psi_{\mathrm{bc}}(y)$ and $\psi''_{\mathrm{bc}}(y)$, respectively. That is,

$$\psi_{\mathrm{bc}}(y) = \sum_{n=0}^{\infty} f_{\mathrm{bc},n}\cos\left(\frac{n\pi y}{b}\right),$$
$$\psi''_{\mathrm{bc}}(y) = \sum_{n=0}^{\infty} g_{\mathrm{bc},n}\cos\left(\frac{n\pi y}{b}\right). \tag{20}$$

Noting that $\psi'_{\mathrm{bc}}(y)$ vanishes at $y=0$ and $y=b$, it can be shown that $g_{\mathrm{bc},k} = -(\frac{k\pi}{b})^2 f_{\mathrm{bc},k}$.

To obtain a finite-dimensional state space model, we retain m axial modes and n transverse modes, and define the $2mn$dimensional state vector

$$\hat{x}(t) \triangleq [\,q_{11}(t) \quad \dot{q}_{11}(t) \quad \cdots \quad q_{mn}(t) \quad \dot{q}_{mn}(t)\,]^{\mathrm{T}}. \tag{21}$$

Then equation (18) can be written in matrix form as

$$\dot{\hat{x}}(t) = A\hat{x}(t) + \hat{B}_1\,\ddot{u}(t) + \hat{B}_2\dot{u}(t), \tag{22}$$

where

$$A = \text{block-diag}\left(\begin{bmatrix} 0 & 1 \\ -\omega_{11}^2 & 0 \end{bmatrix},\ldots,\begin{bmatrix} 0 & 1 \\ -\omega_{mn}^2 & 0 \end{bmatrix}\right), \tag{23}$$

$$\hat{B}_1 = [\,0 \quad b_{1,11} \quad \cdots \quad 0 \quad b_{1,mn}\,]^{\mathrm{T}},$$
$$\hat{B}_2 = [\,0 \quad b_{2,11} \quad \cdots \quad 0 \quad b_{2,mn}\,]^{\mathrm{T}}. \tag{24}$$

To reduce (22) to a state space form with an undifferentiated input, we define a transformed state

$$x(t) \triangleq \hat{x}(t) - \hat{B}_1\ddot{u}(t) - A\hat{B}_1\dot{u}(t) - (A^2\hat{B}_1 + \hat{B}_2)u(t). \tag{25}$$

Hence, it follows from (22) that

$$\dot{x}(t) = Ax(t) + Bu(t), \tag{26}$$

where $B = A^3\hat{B}_1 + A\hat{B}_2 = [\,B_{11} \quad 0 \quad \cdots \quad B_{mn} \quad 0\,]^{\mathrm{T}}$,

$$B_{ij} = -\omega_{ij}^2 b_{1,ij} + b_{2,ij} = \frac{2c^2\rho}{L}\sqrt{\frac{Lb}{4}}f_{\mathrm{bc},j}.$$

Now, consider a pressure sensor at location (x_s, y_s). The measured pressure $y_m(t) = p(x_s,y_s,t)$ is given in terms of the shifted pressure by

$$\begin{aligned} y_m(t) &= p(x_s,y_s,t) = \hat{p}(x_s,y_s,t) + U(x_s,y_s,t) \\ &= \sum_{i=0}^{\infty}\sum_{j=0}^{\infty} q_{ij}(t)V_i(x_s)W_j(y_s) + U(x_s,y_s,t) \\ &= C\hat{x}(t) + U(x_s,y_s,t) \\ &= Cx(t) + CA\hat{B}_1\dot{u}(t) + U(x_s,y_s,t), \end{aligned} \tag{27}$$

where $C \triangleq [\,C_{11} \quad 0 \quad \cdots \quad C_{mn} \quad 0\,]$ with $C_{ij} \triangleq V_{oi}(x_s)W_{oj}(y_s)$. Using the Fourier series identity $1 - \frac{x}{L} = \sum_{i=0}^{\infty}\frac{8}{(2i+1)^2\pi^2}\cos\left(\frac{(2i+1)\pi x}{2L}\right)$, it follows from (16), (19) and (20) that $CA\hat{B}_1\dot{u}(t) = -\rho L(1-\frac{x_s}{L})\psi_{\mathrm{bc}}(y_s)\dot{u}(t) = -U(x_s,y_s,t)$. Hence from (27) we obtain

$$y_m(t) = p(x_s,y_s,t) = Cx(t). \tag{28}$$

Equations (26) and (28) define the state space model of the open duct. The state space model of the speaker-close duct can be obtained by choosing the appropriate shifting function $U(x,y,t)$ and following the analysis presented in this section.

5. Transfer Functions for Two Dimensional Acoustic Duct

In this section we obtain the transfer function of the speaker-open duct from input $u(t)$ to measurement $y_m(t)$ in two ways. Firstly, using the state space model (26), (28), the transfer function for the open duct is

$$G_{\mathrm{open}}(s) = C(sI-A)^{-1}B = \sum_{i=0}^{m}\sum_{j=0}^{n}\frac{s\,C_{ij}B_{ij}}{s^2+\omega_{ij}^2}$$
$$= \sum_{i=0}^{m}\sum_{j=0}^{n}\frac{2c^2\rho}{L}f_{\mathrm{bc},j}\frac{s\cos(\frac{(2i+1)\pi x_s}{2L})\cos(\frac{j\pi y_s}{b})}{s^2+\omega_{ij}^2}. \tag{29}$$

This transfer function is in a *sum-of-modes* form with modal frequencies ω_{ij} and modal residue $R_{ij} = C_{ij}B_{ij}$ for the (ij)th mode.

Authorized licensed use limited to: University of Michigan Library. Downloaded on July 06,2010 at 16:07:56 UTC from IEEE Xplore. Restrictions apply.

A transfer function can also be obtained using temporal Laplace transform of (1). Let $P(x,y,s)$ denote the Laplace transform of $p(x,y,t)$ with respect to t, where s is the Laplace variable. Let $P(x,y,s)$ be of the sererated variable form $P(x,y,s) = X(x,s)Y(y,s)$. The Laplace transform of (1) yields

$$s^2X(x,s)Y(y,s) = c^2(X_{xx}(x,s)Y(y,s)+X(x,s)Y_{yy}(y,s)).$$

For convenience, define $\beta_x^2(s) = \frac{X_{xx}(x,s)}{X(x,s)}$, $\beta_y^2(s) = \frac{Y_{yy}(y,s)}{Y(y,s)}$, so that

$$\frac{s^2}{c^2} = \beta_x^2(s) + \beta_y^2(s). \tag{30}$$

Thus $X(x,s)$ and $Y(y,s)$ are given by

$$\begin{aligned} X(x,s) &= a_1(s)\sinh\beta_x(s)x + a_2(s)\cosh\beta_x(s)x, \\ Y(y,s) &= b_1(s)\sinh\beta_y(s)y + b_2(s)\cosh\beta_y(s)y, \end{aligned} \tag{31}$$

where $a_k(s)$ and $b_k(s)$, $k = 1,2$ are arbitrary constants to be determined.

Substituting (31) in (9) yields $b_1 = 0$ and $\beta_y(s) = \frac{\jmath n\pi}{b}, n = 1,2,\ldots$, where $\jmath = \sqrt{-1}$. We define

$$\beta_{y,n} \triangleq \frac{n\pi}{b}, \quad n = 1,2,\ldots, \tag{32}$$

and hence from (30) we define

$$\beta_{x,k}(s) \triangleq \sqrt{\frac{s^2}{c^2} + {\beta_{y,k}}^2}, \quad k = 1,2,\ldots. \tag{33}$$

Thus the pressure can be written as

$$\begin{aligned} P(x,y,s) = \sum_{n=0}^{\infty} \cos(\beta_{y,n}y)(a_{1,n}(s)\sinh(\beta_{x,n}(s)x) \\ +a_{2,n}(s)\cosh(\beta_{x,n}(s)x)). \end{aligned} \tag{34}$$

Substituting (34) in (7) and (8), operating by $\frac{2}{b}\cos(\beta_{y,k}y)\int_0^b(\cdot)dy$ yields $a_{1,k}(s) = -\frac{\rho\, s\, f_{\mathrm{bc},k}u(s)}{\beta_{x,k}(s)}$ and

$$a_{2,k}(s) = -a_{1,k}(s)\frac{\sinh(\beta_{x,k}L)}{\cosh(\beta_{x,k}L)}. \tag{35}$$

Hence the pressure $P(x,y,s) = G_{\mathrm{irropen}}(s)\,u(s)$, where $G_{\mathrm{irropen}}(s)$ is given by

$$\begin{aligned} &G_{\mathrm{irropen}}(s) = \\ &\sum_{n=0}^{\infty}\cos(\beta_{y,n}y_s)\frac{\rho s f_{\mathrm{bc},n}}{\beta_{x,n}(s)}\frac{\sinh(\beta_{x,n}(s)(L-x_s))}{\cosh(\beta_{x,n}(s)L)}. \end{aligned} \tag{36}$$

Next we compare the irrational transfer function (36) with the transfer functions (29) derived using the state space model. Using the infinite product expansions of $\cosh(x)$ and equations (17), (32) and (33) we can write

$$\begin{aligned} \cosh(\beta_{x,n}(s)L) &= \prod_{r=0}^{\infty}\left[1 + (\frac{2\beta_{x,n}(s)L}{(2r+1)\pi})^2\right] \\ &= \prod_{r=0}^{\infty}\left(\frac{2L/c}{(2r+1)\pi}\right)^2[s^2+\omega_{rn}^2]. \end{aligned} \tag{37}$$

Next we write the partial fractions

$$\frac{\sinh(\beta_{x,n}(s)(L-x_s))}{\beta_{x,n}(s)\cosh(\beta_{x,n}(s)L)} = \sum_{m=0}^{\infty}\frac{l_m s + k_m}{s^2+\omega_{mn}^2}. \tag{38}$$

To determine l_m and k_m, multiply both sides of (38) by the respective sides of (37) and let $s \to \pm\jmath\omega_{mn}$ to obtain $l_m = 0$ and

$$k_m = \frac{2c^2}{L}\cos\left(\frac{(2m+1)\pi x_s}{2L}\right). \tag{39}$$

By substituting (38) and (39) into (36), we obtain the sum of modes transfer function given in (29). Thus the irrational transfer function of the open duct agrees with the transfer function obtained using modal analysis. A similar argument holds for irrational transfer function of the closed duct.

6. Evanescent Waves in State Space Models

In this section we show that the models obtained in previous sections capture the evanescent wave behavior discussed in Section 2.. Let k be an integer such that, for an arbitrary boundary input frequency ω, $\beta_{y,k-1} = \frac{(k-1)\pi}{b} < \frac{\omega}{c} \leq \frac{k\pi}{b} = \beta_{y,k}$. Now, letting $s = \jmath\omega$ and using (32) and (33), note that $\beta_{x,j}(\jmath\omega)$ is real for all $j \geq k$ and purely imaginary otherwise. Each term in the irrational transfer function (36) can be written as

$$T_j(x,y,\jmath\omega) \triangleq Q_j(y,\jmath\omega)\frac{\sin(|\beta_{x,j}(\jmath\omega)|(L-x))}{\cos(|\beta_{x,j}|L)}, j < k \tag{40}$$

$$= Q_j(y,\jmath\omega)\frac{\exp[\beta_{x,j}(L-x)] - \exp[-\beta_{x,j}(L-x)]}{\exp[\beta_{x,j}L] + \exp[-\beta_{x,j}L]}, j \geq k, \tag{41}$$

where $Q_j(y,\jmath\omega) \triangleq \cos(\beta_{y,j}y)\frac{\jmath\rho\omega f_{\mathrm{bc},j}}{\beta_{x,j}}$. Here $\beta_{x,j} \equiv \beta_{x,j}(\jmath\omega)$. For $j \geq k$, it can be seen that $T_j(x,y,\jmath\omega)$ decays exponentially to zero as $x \to L$ and for $j < k$, $T_j(x,y,\jmath\omega)$ is sinusoidal, thus a propagating solution in x. For a semi-infinite duct (as in section 2.), $\beta_{x,j}(\jmath\omega)L \gg 1$ hence $T_j(x,y,\jmath\omega) \approx Q_j(y,\jmath\omega)e^{-\beta_{x,j}(\jmath\omega)x}$ for $j \geq k$.

Comparing these analytical results with the theory in section 2. it is apparent that $T_k(x,y,\jmath\omega)$ corresponds to the eigenfunction $p_k(x,y,t)$ and $c\beta_{y,k} = \omega_{\mathrm{co},k}$ is the 'cut-off' frequency for $T_k(x,y,\jmath\omega)$. The fundamental mode, hence, is described by $T_0(x,y,\jmath\omega)$.

Moreover if $\psi_{\mathrm{bc}}(y)$ such that its first Fourier coefficient $f_{\mathrm{bc},0} = 0$ and if $\omega \leq \omega_{\mathrm{co},1}$ then all the term in the summation (36) decay to zero exponentially as $x \to L$. Consequently there is no sound propagation in the duct or waveguide. This is the global cut-off frequency (5) defined in Section 2.. However if $f_{\mathrm{bc},0} \neq 0$ then only the fundamental mode $T_0(x,y,\jmath\omega)$ is propagated. This is in accordance with the behavior discussed in Section 2. and hence the irrational transfer function (36) does capture the cut-off phenomenon. The angle θ defined in (6) can be shown to

Authorized licensed use limited to: University of Michigan Library. Downloaded on July 06,2010 at 16:07:56 UTC from IEEE Xplore. Restrictions apply.

be the same as the angle between the propagation vector $\vec{\beta} \triangleq \beta_{x,k}\hat{\imath} + \beta_{y,k}\hat{\jmath}$ and the x direction.

As an example, consider a duct 5 m long and 0.15 m wide. For simplicity, consider a boundary input such that $\psi_{\rm bc}(y) = \cos(2\pi y/b)$ so that $f_{{\rm bc},k} \neq 0$ only if $k = 2$. The summation in (36) then reduces to a single term $T_2(x, y, \jmath\omega)$ which is plotted as a function of ω for several values of sensor location $x_{\rm s}$ (see Figure 1(a)). Below the cut-off frequency $\omega_{{\rm co},2}$, as $x_{\rm s} \to L$, $T_2(x, y, \jmath\omega) \to 0$. However resonant peaks are observed above the cut-off frequency.

A comparison of sum-of-modes transfer function (29) and (36) is plotted in Figure 1(b). The plot shows the magnitude of sum-of-modes transfer function with $m = 100, 1500$ for sensor located at $x_{\rm s} = L/5$. Although the sum-of-modes transfer function agrees well beyond the cut-off frequency, there is a disparity of orders of magnitude below the cut-off frequency. This is because an exponential solution cannot be approximated by a finite sum of sinusoids. However it is observed that the sum-of-modes transfer function does show evanescent behavior as $x_{\rm s} \to L$.

In summary, in this paper we develop state space models for a two-dimensional acoustic ducts using modal decomposition of the response to an arbitrary boundary input issued by a speaker located at one end of the duct. This paper also derives irrational transfer functions using Laplace transforms which exactly capture the cut-off phenomenon or the evanescent wave behavior observed in acoustic ducts. The *sum-of-modes* transfer functions derived from the state space models are shown to agree with the irrational transfer functions. Note, however, that a one-dimensional acoustic model which essentially is the fundamental $T_0(x, y, \jmath\omega)$ is insufficient to capture the evanescent behavior.

References

[1] A. H. von Flotow and B. Schäfer, "Wave-Absorbing Controllers for a Flexible Beam," *J. Guid. Contr. Dyn.*, Vol. 9(6), pp. 673-680, Nov.-Dec. 1986.

[2] K. F. Graff, *Wave Motions in Elastic Solids.* New York: Dover Publications, 1975.

[3] A. J. Hull, C. J. Radcliffe, M. Miklavcic and C. R. MacCluer, "State Space Representation of the Nonself-Adjoint Acoustic Duct System," *Journal of Vibration and Acoustics,* Vol. 112, pp. 483 - 488, 1990.

[4] L. E. Kinsler, A. R. Frey, A. B. Coppens and J. V. Saunders, *Fundamentals of Acoustics.* New York: John Wiley, 1982.

[5] D. W. Miller and A. H. von Flotow, "Traveling Wave Approach to Power Flow in Structural Networks," *Journal of Sound and Vibration,* Vol. 128(1), pp. 145-162, Jan. 1989.

[6] P. M. Morse and K. U. Ingard, *Theoretical Acoustics.* Princeton: Princeton University Press, 1986.

[7] A. D. Pierce, *Acoustics: An Introduction to its Physical Principles and Applications.* New York: Acoustical Society of America, 1991.

[8] C. J. Radcliffe and S. D. Gogate, "Identification and Modeling of Speaker Dynamics for Acoustic Control Applications," *Active Control of Noise and Vibrations, ASME,* Vol. 38, pp. 295 - 300, 1992.

[9] R. Venugopal and D. S. Bernstein, "State Space Modeling of Acoustic Duct with End-Mounted Speaker," *Proc. of Conference in Control Applications,* Dearborn, MI, Sept. 1996, pp. 954 - 959.

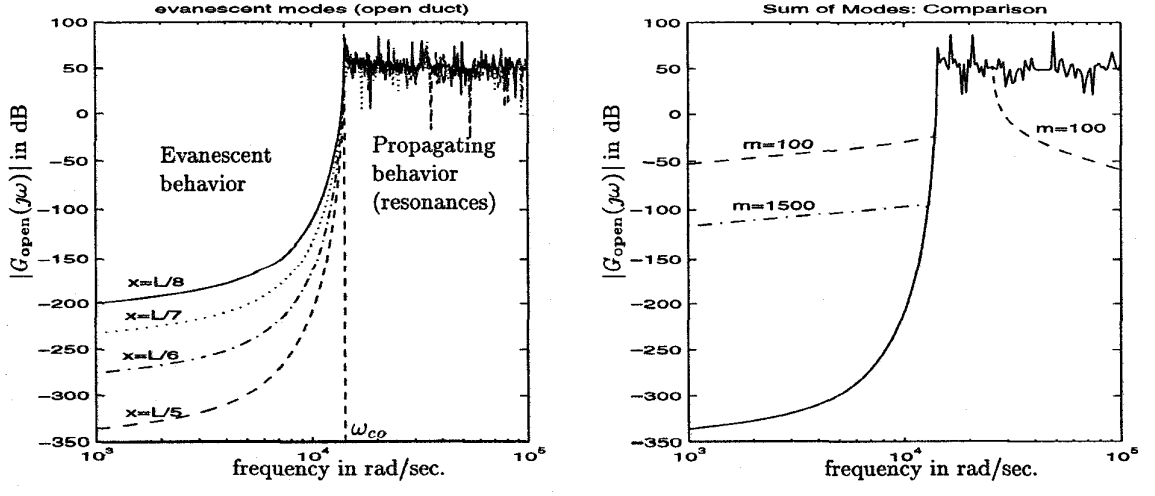

Figure 1: (a) Magnitude plots of the transfer function (36) for different values of $x_{\rm s}$. (b) Comparison of transfer functions (29) and (36).

Authorized licensed use limited to: University of Michigan Library. Downloaded on July 06,2010 at 16:07:56 UTC from IEEE Xplore. Restrictions apply.